FINITE ELEMENT ANALYSIS OF FATIQUE BEHAVIUOR OF RAILWAY NETWORK MATERIALS

Prof. M.Sc. Maier C. PhD.[1], Duchambon M. Engineering student[2],
Faculty of Mechanical Engineering –University Dunarea de Jos of Galati, Romania[1]
Ecole des Mines de Douai, France [2]

Abstract: *Railway networks are subjected to severe and various loading conditions. In service, crossings are submitted to rolling, impact and sliding stress affecting their fatigue behaviour. Experimental and numerical simulation in laboratory is a convenient research technique to test a large number of contact parameters and theirs influence on the fatigue behaviour of the material. For this reason the present paper propose a numerical tool designed using finite element method and simulating the impact-sliding test, one of specific test for this kind of study. The results are described and discussed and shows the influence of contact parameters on the: size and shape of the contact area, maximal values of the equivalent Von Mises stress and plastic strain, depth of the equivalent Von Mises stress propagation.*

Keywords: RAILWAY NETWORKS, FINITE ELEMENT SIMULATION, IMPACT-SLIDING TEST, CONTACT PARAMETERS

1. Introduction

Switches and crossings are important elementes in a railway network as they provide flexibility to trafic operations. They consist in a switch and a crossing panel connected by a clossure panel. In the crossing panel, there is a discontinuity in the rail, which leads to high dynamic loads. The process of a wheel passing a crossing panel is highly complex, including dynamic effects with contact and complex geometries. The principal damage mechanisms affecting switches and crossings components, are: wear, accumulated plastic deformation and rolling contact fatigue. In order to study and predict all these mechanisms different tests are designed, performed and simulated. In the development of new concepts or in the improvement of existing ones, numerical models can help to shorten development times. This can be done both by predicting the performance of possible design concepts and improving the understanding of the mechanisms of loading. Many studies are provided on this subject.

A. Ramalho, M. Esteves and P. Marta [1] investigate the effect of contact conditions on friction and wear behaviour of carbon and low alloy rail/wheel steels. Two-disc rolling-sliding tests were done to study the effect of the creep ratio, contact pressure and tangential speed on the resulting traction coefficient and amount of wear. Scanning and optical microscopy and the evolution of micro hardness were used to observe contact surface and to evaluate the strain-hardening effect induced by contact stresses. M. Pau, B. Leban and A Baldi [2] report the results of a series of experiments performed on realistic wheel-rail coupling, in which the wheel was characterized by the presence of subsurface defects.

Experimental and numerical modeling of wheel-rail contact and wear is reported [3] by A. Rovira, A. Roda, M.B. Marshall, H. Brunskill and R. Lewis. An experimental method, based on the measurement of ultrasonic reflection, is used to solve the contact problem, together with a simplified theory of rolling contact algorithm.

M. Peltz, W. Daves and H. Ossberger propose a dynamic finite element model for the process of a wheel passing the crossing panel of a turnout [4]. The model provides the dynamical contact forces between the wheel and the crossing parts, the vertical wheel displacement, the development of the angular velocity of the wheel, the stress fields and the plastic deformation in the crossing, the contact pressure and the microslip. Numerical simulation results of wheel rolling over rail at high-speeds [5] are obtained by Jiang X. and Jin X. considering the rolling contact of the wheel and rail as a two-dimensional rolling contact in a pure rolling and steady state. Three-dimensional elastic-plastic stress analysis of wheel-rail rolling contact [6], using ABAQUS, was performed by Z. Wen, L. Wu, X. Jin and M. Zhu. The finite element simulations were conducted to investigate the influence of partial slip condition and varying contact load on the rolling contact stresses and deformations. Impact and sliding wear resistance of Hadfield and rail steel are studied [7] by R. Harzallah, A. Mouftiez, E. Felder, S. Hariri and J.-P. Maujean. The influence of contact parameters on the damage of different materials was investigated byimpact and impact-sliding tests.

The large contact forces between wheel and rail, causing severe damages at the crossing noses, represents the reasons way great efforts should be taken in decreasing the dynamic response. The current research paper present a numerical model of the specific rig test used to perform impact sliding contact tests at the "Ecole des Mines" of Douai, France (fig.1).

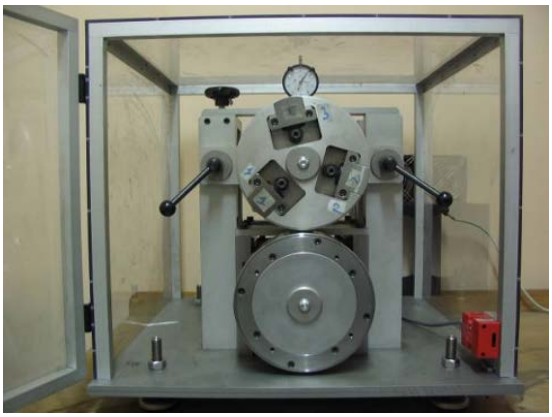

Fig. 1 *Impact sliding tribotester*

This test rig is used to study the consequences of repeated impacts and sliding of a specimen made in the metal to test. The specimen is a metallic pawn-shaped part of 10 mm diameter and 27 mm in length.

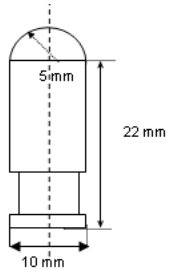

Fig 2 *Geometry of the specimen*

This test rig is made of two rotating discs; the specimen can be fixed on the upper disc (three specimens, at most, can be studied at the same time). During the rotation of the discs, the specimens

impact the lower disc because of the centrifugal load created on them by the rotation of the upper disc.

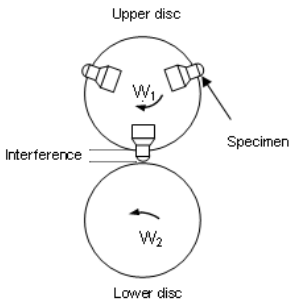

Fig. 3 *Plan of the test rig*

2. Numerical simulation

The numerical simulation of the test rig is performed using MARC Mentat finite element code.

For the meshing of the specimen, two different techniques are used. Starting from the in the plane Oxy meshed with quadratic elements specimen, and then expanding by rotation to get the whole specimen, it results a hexahedral elements meshing (fig. 4). However, this meshing presents some degenerate elements (tetrahedral elements at the bottom of the specimen), which can lead to mistakes in the computation.

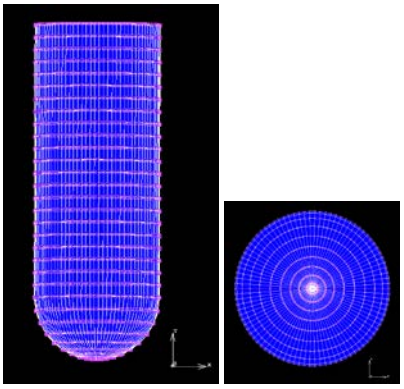

Fig. 4 *Hexahedral meshing of the specimen*

To prevent this, another meshing technique is used: representing the specimen as a solid, and then meshing its surface with triangular elements, finally results a tetrahedral elements meshing (fig. 5).

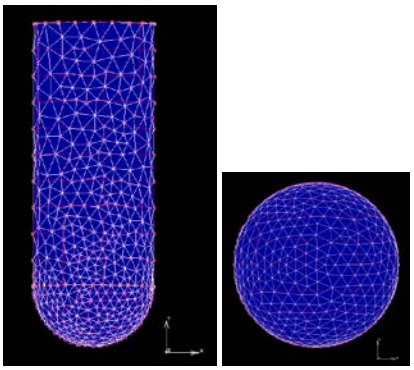

Fig. 5 *Tetrahedral meshing of the specimen*

The considered material of the specimen is a HSLA steel (High-Strength Low-Alloyed steel), which coefficients for the Swift's law (equation 1) are: A=673, m=0.131.

$$\sigma_0 = A\,(\varepsilon_0+\varepsilon)^m \qquad (1)$$

In all the different models, the test rig is represented by the specimen and the lower disc. The specimen is considered as a deformable body, and the disc as a rigid body. A face load equivalent to the centrifugal force, which results from the rotation of the upper disc, is applied to the upper surface of the specimen; the specimen is also free for the displacements in the radial direction. In order to define boundary conditions four models are studied.

In the first model, the specimen is fixed, and the disc is in rotation, with a speed equal to the sum of the rotation speeds of the two discs. The centre of rotation is align with the axis of the specimen.

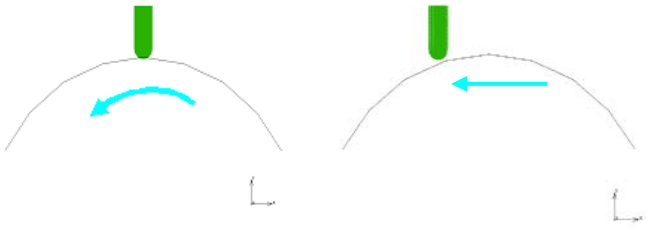

Fig. 6 *First and second model*

This model can be used to study the behavior of the specimen during the contact between the disc and the specimen, but it doesn't consider the impact between the specimen and the disc.

In the second model, the specimen is fixed, and the disc is in translation, with a speed equal to the linear speed of contact between the specimen and the disc.

In the third model, the specimen is fixed, and the disc is in rotation, like in the first model, but in this model, the centre of rotation of the disc is not align with the axis of the specimen, in order to create an impact between the two parts.

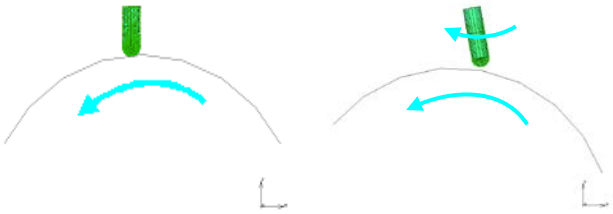

Fig. 7 *Third and forth model*

In the forth model, both the specimen and the disc are in rotation. In order to enable the rotation of the specimen, it is necessary to add another rigid body, which will be in contact with the specimen and will guide its rotation. The contact type "glue" which behaves as if the two parts were glued together, can not be used in this situation, because it would block the displacement of the specimen in the radial direction, and the load equivalent to the centrifugal force would also have no influence.

The three first models can't be used to study the case without sliding, in which the sliding velocity between the specimen and the disc is null (the disc and the specimen have the same velocity).

Therefore, we have decided to use the forth model, which is closer to the way the test rig works, and can also be used to study the case without sliding.

To improve this model, different types of surfaces, guiding the rotation of the specimen, are tested and the cylinder provides the best rotation for the specimen.

The test rig can be use with or without sliding.

In the case without sliding, the two discs have the same rotational speeds, and there is no friction coefficient between the lower disc and the specimen.

In the case with sliding, the two discs have different rotational speeds, and there is a friction coefficient between the parts. Based on the thesis, I have set two different values for the friction coefficient: μ=0.4 and μ=1.

The values for the rotational speeds of the discs are 300 rot/min, 200 rot/min or 100 r/min (for the lower disc); the rotational speed of the disc influences the centrifugal load on the specimen (represented as a face load on the upper surface of the specimen). The sliding speed between the two discs is 0 m/s or 1 m/s. The 6 different cases studied are presented in table 1.

***Table 1**: Test parameters for different cases studied*

	Parameters								
	ω1 (rot/min)	**ω2 (rot/min)**	**μ**	**Force (N)**	**F/surface (N/mm²)**	**speed1 (rad/s)**	**speed2 (rad/s)**	**sliding speed (m/s)**	**time (s)**
Case without sliding	300	300	0	4.44106	0.0565	31.42	31.42	0	0.011
	200	200	0	1.97380	0.0251	20.94	20.94	0	0.017
Case with sliding	300	200	0.4	4.44106	0.0565	31.42	20.94	1	0.011
	200	100	0.4	1.97380	0.0251	20.94	10.47	1	0.017
	300	200	1	4.44106	0.0565	31.42	20.94	1	0.011
	200	100	1	1.97380	0.0251	20.94	10.47	1	0.017

The parameters we have to change in the model are the rotational speeds of the discs (in rad/s), the surface force, the friction coefficient and the time.

3. Results and conclusions

For each case, the maximum value of the equivalent Von-Mises stress and of the plastic strain, the depth of stress propagation, such as the dimensions of surface contact are presented in the table 2.

***Table 3:** Test results for the different studied cases*

	Parameters			Results					
	ω1 (r/min)	**ω2 (r/min)**	**μ**	**max stress (MPa)**	**plastic strain**	**stress depth (mm)**	**2a (mm)**	**2b (mm)**	**surface (mm²)**
Case without sliding	300	300	0	445.4	0.04438	0.9735	1.2480	1.0764	1.05512
	200	200	0	443.3	0.04319	1.4925	1.2480	1.0452	1.02453
Case with sliding	300	200	0.4	473.7	0.06819	1.1765	1.6381	1.2012	1.54540
	200	100	0.4	470.2	0.06464	1.2181	1.6381	1.1856	1.52533
	300	200	1	512.3	0.1246	3.3696	2.0749	1.3573	2.21173
	200	100	1	516.8	0.1331	2.1369	2.0437	1.3417	2.15343

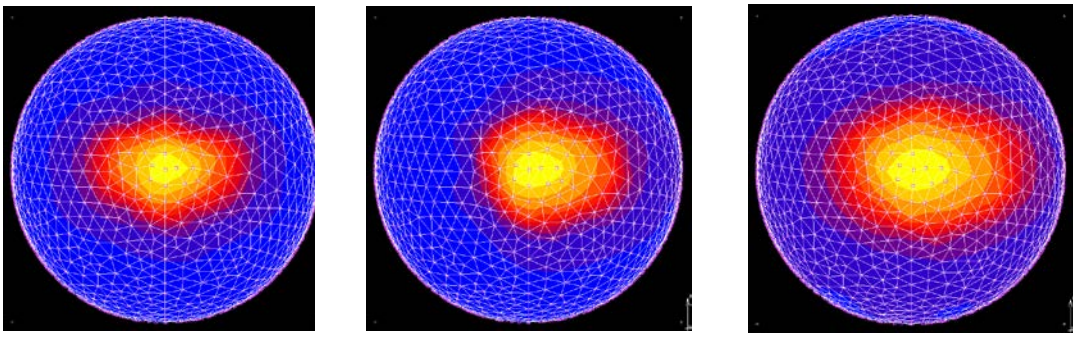

***Fig. 8** Representation of the Von-Mises stress on the specimen for the cases: without sliding, with sliding and μ=0.4, with sliding and μ =1*

For each couple of force within a same case, the values are close. Therefore, we are going to consider only the results found for a rotational speed of 300 rot/min.

The stress, plastic strain and surface' values are higher for the cases with sliding than for the cases without sliding, and within the cases with sliding, those values increase with the friction coefficient.

The central spot of the diagram (corresponding to the higher value for Von-Mises stress), is bigger for the cases with sliding, and is the biggest for the case with the higher friction coefficient. The contact area also has a more circular and centered shape for the case without sliding, but changes to an elliptical shape for the cases with sliding.

It is observed that the equivalent Von-Mises stress propagation goes deeper in the case with sliding that in the case without sliding, and within the case with sliding, and the depth increases with the friction coefficient.

Examination of the results shows large plastic deformation in surface and subsurface of specimen. In comparison with impact tests, sliding produces a change in size and shape of the contact area, a weight loss and lower hardening.

Results obtained with the numerical tool, proposed in this paper, are confirmed by experimental and numerical results obtained by different researchers. Only the force (which is determined by the rotational speed of the upper disc) influence on the results, is not confirmed. In ours case, the force has only little influence on the results in comparison with conclusions reported by other researchers. This might be due to the approximation made in the definition of the material. In order to improve the precision of this numerical tool, mechanical behaviour of the material can be provided by introducing real $\sigma - \varepsilon$ curve obtained from tensile test.

The proposed numerical tool can help to shorten development of new concept, improvement of existing ones or prediction of the performance of possible design concepts of switches and crossings panels. This numerical model assures a good precision of the results in comparison with experimental procedure.

References

[1] A. Ramalho, M. Esteves, P. Martha, Friction and wear behaviour of rolling-sliding steel contacts, Wear (2013), http://dx.doi.org/10.1016/j.wear.2012.12.008, p. 1-13.
[2] M. Pau, B. Leban, A. Baldi, Simultaneous subsurface defect detection and contact parameter assessment in a wheel-rail system, Wear 265 (2008), p. 1837-1847.
[3] A. Rovira, A roda, M.B. Marshall, H. Brunskill, R. Lewis, Experimental and numerical modeling of wheel-rail contact and wear, Wear 271 (2011), p. 911-924.
[4] M. Peltz, W. Daves, H. Ossberger, A wheel set/crossing model regarding impact, sliding and deformation-Explicit finite element approach, Wear 294-295 (2012), p. 446-456.
[5] Jiang Xiaoyu, Jin Xuesong, Numerical simulation of wheel rolling over rail at high-speeds, Wear 262 (2007), p. 666-671.
[6] Wen Zefeng, Wu Lei, Li Wei, Jin Xuesong, Zhu Minhao, Three-dimensional elstic-plastic stress analysis of wheel-rail rolling contact, Wear 271 (2011), p. 426-436.
[7] R. Hazallah, A. Mouftiez, E. Felder, S. Hariri, J.-P. Maujean, Rolling contact fatigue of Hadfield steel X120Mn12, Wear 269 (2010), p. 647-654.
[8] X.S. Jin, W.H. Zhang, J. Zeng, Z.R. Zhou, Q.Y. Liu, Z.F. Wen, Adhesion experiment on a wheel/rail system and its numerical analysis, J. Eng. Tribol. 218 (2004) 293–303.
[9] S. Damme, U. Nackenhorst, A. Wetzel, B. Zastrau, On the numerical analysis of the heel-rail system in rolling contact, in: K. Popp, W. Schielen (Eds.), System Dynamics and Long-term Behavior of Railway Vehicles, Track and Subgrade, Springer, Berlin, Heidelberg, 2003, pp. 155– 174.